Desalination and Water Treatment
www.deswater.com

doi:10.5004/dwt.2016.0129

61 (2017) 88–97
January

Preparation of cellulose triacetate forward osmosis membranes for treating esterification wastewater

Quanju Ji[a], Zheng Lv[a], Yanbin Yun[a,*], Jianbo Li[b], Chunli Li[c,*], Shouwei Zhu[d]

[a]*School of Environmental Science and Engineering, Beijing Forestry University, Beijing, 100083, China, email: quanju_ji@126.com (Q. Ji), 705641517@qq.com (Z. lv), yunyanbin@bjfu.edu.cn (Y. Yun)*
[b]*Faculty of Modern Agricultural Engineering, Kunming University of Science and Technology, Kunming, 650500, China, email: jianbo69@sina.cn*
[c]*New Technique Centre, Institute of Microbiology, Chinese Academy of Sciences, Beijing, 100101, China, email: licl@im.ac.cn*
[d]*Hyflux Filtech Co., Ltd. Shanghai, 201700, China, email: shouwei_zhu@hyflux.com*

Received 30 January 2016; Accepted 29 May 2016

ABSTRACT

Cellulose triacetate (CTA) membranes for forward osmosis (FO) were prepared by phase inversion. Effects of the polymer concentrations, solvents (1,4-dioxane, N-methylpyrrolidone, N, N-dimethylformamide), additives (lactic acid and PVP-K30) on the FO membrane performance and gelation kinetics mechanism were explored. The pre-treated esterification wastewater was further treated via the optional membrane under the FO mode, the long-term FO performance and fouling behaviors of CTA membranes are further investigated. Results showed that the CTA membrane cast using 1,4-dioxane as solvent has shown lower water flux but higher salt rejection, whereas the membrane cast using N-methylpyrrolidone or N, N-dimethylformamide as solvent has excellent permeability but poor selectivity. The water flux and reverse salt flux reduced with the increase of CTA concentration. As the lactic acid and PVP-K30 increased, the gelation velocity accelerated, the water flux and reverse salt flux enhanced. Furthermore, the water flux went down significantly by 51.1% in the long-term test. Especially in the early 5 h, the flux declined sharply from 9.56 LMH to about 6.0 LMH, and then the water flux reduced slowly since the membrane fouling become to stability. FO treatment brought about 57.1% of water recovery and favorable pollutants rejection with TOC rejection exceeding 96%.

Keywords: Cellulose triacetate; Forward osmosis; Gelation kinetics; Esterification wastewater

1. Introduction

Esterification wastewater generated by esterification reaction generally stems from polyester production process in chemical enterprise [1,2]. Its water quality characteristics include: (1) complicated component and high chroma; (2) high organic contents with aromatic compounds; (3) low biodegradability; (4) high corrosivity and toxicity. Therefore, if discharged directly into the water, the esterification wastewater will threaten the environment and human health [1,2,4]. It is essential to strengthen the treatment for esterification wastewater based on the green environmental protection concept [3]. Traditional treatment methods for esterification wastewater are limited to biochemical treatment and physicochemical treatment, high investment and operation cost, low purification efficiency and unstable effluent were prominent defects [1–3]. Therefore, an effective and applicable technique to treat esterification wastewater needs to be developed.

Recently, as a new membrane separation technology, forward osmosis (FO) is drawing increasing attention. FO is a membrane separation process which employs osmotic pressure difference to transport water through a semipermeable membrane [5]. Some apparent advantages such as lower energy consumption, high anti-polluting and strong

---

*Corresponding authors.

Presented at the 6th IWA-ASPIRE Conference & Exhibition, Beijing, China, 20-24 September 2015.

membrane reproducibility has attracted growing attention in application to wastewater treatment [6,7,8].

As early as the 1980s, Anderson and Votta [9] had proposed the feasibility of using FO for industrial wastewater. Recently, Coday et al. [9] conducted an weeklong field test that revealed the FO system recovered 85% of drilling wastewater by concentrating it five times. Gebreyohannes et al. [10] employed FO to dehydrate olive mill wastewater, and obtained more than 98% rejection to those components. Zhao et al. [11] investigated the FO performance when used to treating the surfactant wastewater. A satisfactory result showed the surfactant rejection can be as high as 99.77% and the water flux was more than 8.0 L m^{-2} h^{-1}. Besides, the FO process was also used for dye wastewater treatment by Zhao et al. [12], the influence of draw solution (DS) temperature on FO performance was also investigated. It is worth noticing that the FO performed well at higher temperatures (45°C). Kumar and Pal [13] developed a novel FO-nanofiltration system for treating coke wastewater and the effects of DS on the water flux and rejection of target contaminants were studied. When the DS was determined to be 1.5 M NaCl, about 96~98% rejection of contaminants could be obtained along with the water flux of 46 L m^{-2} h^{-1}. In addition, Dong et al. [14] used a FO membrane system to post-treat the effluent of membrane bioreactor disposing of landfill leachate and found about 98.6% of COD was achieved. Direct filtration for municipal wastewaters by triacetate acetate (CTA) FO membrane supplied by hydration technology innovations (HTI) was also investigated and showed a satisfactory flux of 3~7.4 L m^{-2} h^{-1} [15].

Desirable FO membranes are one of the key technologies of FO wastewater process that also is the current research focus. Nguyen et al. [16] develop triacetate/cellulose acetate (CTA/CA) FO membrane casting from CTA/CA, 1,4-dioxane, acetone, and methanol as solvent, maleic acid as additives. It was obtained that 10.39 L m^{-2} h^{-1} water flux and 0.084 mol m^{-2} h^{-1} NaCl. Sairam et al. [17] prepared CA FO membranes with lactic acid, maleic acid and zinc chloride ($ZnCl_2$) as pore-forming agents. And the membranes prepared with $ZnCl_2$ gave 5.5 L m^{-2} h^{-1} water flux and a NaCl rejection of 95% in FO runs. Yip et al. [18] developed a type of membranes consisting of a selective polyamide active layer formed by IP on top of a polysulfone (PSF) support layer. The water fluxes exceeded 18 L m^{-2} h^{-1}, while the salt rejection maintained more than 97% when using a 1.5 mol L^{-1} NaCl draw solution. Setiawan et al. [19] developed a type of hollow fiber FO membrane with a positively charged nanofiltration-like membrane by polyelectrolyte post treatment for apolyamide-imide (PAI) substrate using polyethyleneimine (PEI). The water flux was 9.74 L m^{-2} h^{-1}, and the J_S/J_V is lower than the data of 0.85 g L^{-1} for commercial FO membrane from HTI.

It was observed that different materials were used for FO membranes [20]. As a kind of widely used membrane material, CTA had significant advantages such as higher hydrophilicity and the simple fabrication process (one step forming) of FO membranes [21]. Furthermore, CTA membranes have superior resistance toward chlorine comparing to the polyamide-based thin film composite membranes [22]. CTA is also insensitive to thermal, chemical, biodegradation and hydrolysis. Above special advantages make CTA a good candidate as a FO material [8,22]. So far, the literature relevant to CTA FO membranes is few which illustrates there's more unknown territory to explore such as the choice of solvents, additives as long as formation conditions.

Therefore, this paper aims to study the functional mechanism toward the fabrication of CTA FO membranes by using different solvent such as 1,4-dioxane, N-methylpyrrolidone (NMP), N, N-dimethylformamide (DMF), additives (lactic acid and PVP-K30). Kinetic experiments were first applied to explore gelation kinetics mechanism in this study. The effects of the polymer concentrations, solvents and additives on FO membrane performances and gelation kinetics mechanism were investigated in detail. The optional membrane was used in treating esterification wastewater under the FO mode. The long-term FO performance such as water flux, contaminants rejection and fouling behaviors of CTA membranes are further investigated.

2. Materials and methods

2.1. Chemicals

Cellulose triacetate (CTA) was supplied by Eastman Chemical Company, USA. 1,4-dioxane (≥99.5% purity) and Sodium chloride (NaCl, 99.0% purity) were purchased from Sinopharm Chemical Reagent Co., Ltd. N-methyl pyrrolidone (NMP, ≥99.0 purity) and lactic acid (85.5~90.0% purity) were from Xilong Chemical Industry Co., Ltd. N, N-dimethyl formamide (DMF, ≥99.5%) and D-Glucose ($C_6H_{12}O_6{\cdot}H_2O$) were from Beijing Chemical Works. Polyvinylpyrrolidone (PVP-K30, ≥95.0% purity) was purchased from Beijing Lanyi Chemical Products Co., Ltd. All solvents were AR (analytical reagents) grade and used without further purification.

2.2. Membrane preparation

CTA membranes for forward osmosis were prepared by phase inversion. CTA polymer and additives were dissolved in solvents in the conical flask with stopper that was well-sealed by sealing film in order to prevent evaporation of solvents. Magnetic Stirrer was used to stir the mixture thoroughly until a homogeneous dope solution formed. A clean and dry glass plate was attached to flat workbench by strong tape. Then, the homogenized solution was cast on glass plate using a casting knife at room temperature. After volatilizing the solvent for 30 s, the coating attached on glass plate were soaked in coagulation to solidify. All new membranes were immersed in deionized (DI) water for 24 h with the purpose of further removing the residual solvent. Finally, the membranes were kept in DI water for stand-by and annealed in DI water for 15 min at 60°C before testing performance. All compositions of casting solution used in this paper were showed in Table 1.

2.3. Kinetic experiments

The gelation process of casting solution was determined using a high-precision inverted microscope (BDS-200PH, Chongqing OPTEC Instrument Co., Ltd, Chongqing, China) with an image real-time storage system. Its technical parameters of microscope were fixed to WF10X/20 and LPL 10/0.25 W. D. When the microscope was ready, a drop of the

Table 1
The composition of casting solution

Membrane	Composition (wt.%)					
	CTA	1,4-dixane	DMF	NMP	Lactic acid	PVP-K30
1	11.7	79.58			6.92	1.8
2	11.7		79.58		6.92	1.8
3	11.7			79.58	6.92	1.8
4	12.0	84.0			4.0	
5	13.0	83.0			4.0	
6	14.0	82.0			4.0	
7	15.0	81.0			4.0	
8	16.0	80.0			4.0	
9	17.0	79.0			4.0	
10	18.0	78.0			4.0	
11	15.0	85.0			0	
12	15.0	84.0			1.0	
13	15.0	83.0			2.0	
14	15.0	82.0			3.0	
15	15.0	81.0			4.0	
16	15.0	80.0			5.0	
17	15.0	79.0			6.0	
18	15.0	81.0			3.0	1.0
19	15.0	80.5			3.0	1.5
20	15.0	80.0			3.0	2.0
21	15.0	79.5			3.0	2.5
22	15.0	79.0			3.0	3.0

casting solution was placed on a glass slide, which was covered by another slide specially designed. Then a drop of the DI water was introduced from the holes in the second glass and ensure the casting solution droplet between two slides was surrounded by the DI water, and then the gelation process was initiated soon. The whole gelation process was then recorded with the optical system. Professional image processing software was used for processing the resulting images, determining the precipitation rate [25].

2.4. Performance testing of FO membranes

The membranes were tested at room temperature by a self-made FO device (Fig. 1) that includes a membrane module with 40 cm^2 (length, 10 cm; width, 4 cm) effective area, and its active layer faced FS. FS tank with 1 L DI water was placed on magnetic stirrer for stirring. A conductivity meter (DDS-307, Shanghai INESA Scientific Instrument Co., Ltd, Shanghai, China) was used to determine NaCl concentration. Draw solution (DS) tank equipped with 1 L 1 mol L^{-1} NaCl was placed on an electronic balance (HZT-A2000, Huazhi Scientific Instrument Co., Ltd, Fujian, China) for recording DS quality change. The FS and DS were circulated on each side of the membrane at a cross-flow rate of 1 L min^{-1}, which was controlled by flow meter and magnetic pumps (MP-20RM, Shanghai Xinxishan industrial Co., Ltd). All experimental tests were conducted under the FO mode.

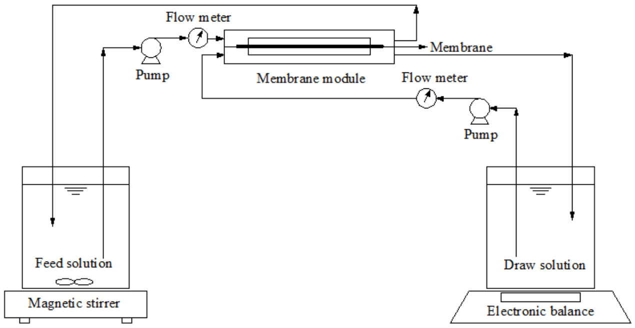

Fig. 1. Laboratory-scale forward osmosis testing device.

The water flux (J_w) and the reverse salt flux (RSF, J_s) were assessed by running the device for 1 h after system stability. Experimental data was recorded every 10 min.

The water flux (J_w, L m^{-2} h^{-1}) was refers to the volume of pure water transferred from FS to DS per unit area and per unit time, which was calculated as follows: $J_w = \Delta W/\rho A\Delta t$. Where, ΔW (g) is the quality of pure water passing through the membrane, ρ (kg m^{-3}) is the density of water, A (m^2) is the available membrane area, Δt (h) is the effective testing time. The RSF (J_s) was defined as the quality of NaCl diffusing from the DS to the FS per unit membrane area per unit time. It was calculated as follows: $J_s = m_s/A\ \Delta t$. Where, m_s is the quality of the NaCl diffused across the membrane per unit area during the 1 h tests, A (m^2) is the available membrane area, Δt (h) is the effective testing time. The salt quality was calculated by using the standard curve established before experiments.

2.5. Other analysis indicators

2.5.1. Automatic surface tensiometer

Surface tensions of drop solutions were determined by automatic surface tensiometer (JYW-200A, Chengde Jinhe Instrument Manufacturing Co., Ltd, Hebei, China) using platinum ring method. The sample stage moved up and down by buttons and results were displayed automatically.

2.5.2 Rotary viscometer

Viscosities of casting solutions were measured using rotary viscometer (NDJ-1, Shanghai Changji Co., Ltd., Shanghai, China) at room temperature. Four rotors and four different rotational speeds were provided. Any combination of rotor and rotational speed can be free to choose as required.

2.5.3 Scanning electron microscopy (SEM)

Surface and cross-section imagines were observed using scanning electron microscopy (SEM, FEI, Quanta 200, Holland). Each sample was cut in liquid nitrogen at first and then fixed on a specimen stage using carbon conductive adhesive tape. In order to improve the image formation quality, the samples were coated with platinum prior to observing the morphology.

2.5.4 *Contact angle instrument*

Contact angle of membranes was determined by contact angle instrument (JY-PHa, Chengde Jinhe Instrument Manufacturing Co., Ltd, Hebei, China) using sessible drop method. Dried sample was assembled on a slide with double-sides tape, and then put on objective table. Change the focal length and obtained a clear image. DI water (about 2.5 μL) was forced out so that the formation of a liquid droplet on the needle. Then, sample was contacted with liquid droplet by moving up the objective table. At this time, the moment that liquid droplet drop down, the membrane was recorded through imaging system. And the contact angle was measured using the ellipse fitting method by software.

2.6. *Application of CTA FO membranes in treating esterification wastewater*

The esterification wastewater used in experiments was supported by Beijing Chemical Industry Group Co., Ltd, which contains large amounts of non-degradation organic compound. This study aims to concentrate the wastewater and evaluate the pollutants removal efficiency by FO membrane.

2.6.1. *Esterification wastewater pre-treatment*

For reducing the membrane fouling, the esterification wastewater was pretreated before flowing into FO system by two different pre-treatment methods: (1) Flocculation-precipitation (by adding 6.0 mg L^{-1} poly aluminium chloride and standing for 120 min) to eliminate a mass of glue and some organic matters; (2) Filtration through 1~3 μm pore size qualitative filter paper to further remove the residual floc in process (1). Details of the esterification wastewater such as pH, TDS, TOC after pretreatment were measured.

2.6.2. *Water reclamation from wastewater*

The effluent leaving pre-treatment unit was further treated by a lab-scale cross-flow FO unit to retain and fractionate the pollutants. The test was conducted under the FO mode where the membrane active layer faces the esterification wastewater. During the test for up to 24 h, the concentration of NaCl (1 L) acted as draw solution was maintained to be 2 M, while in order to clarify the fouling behaviors of membrane during the wastewater treatment, the feed solution was either 1 L esterification wastewater or DI water. The flow rate on both side of the membrane was kept at 0.3 L min^{-1}, the temperature of feed solution and draw solution was maintained at 25 °C.

2.6.3. *Esterification wastewater characterization*

Wastewater properties before and after treatment were characterized according to the following items:

Total organic carbon (TOC): was determined by TOC analyzer (TOC-Vcsn, Shimadzu Corporation, Japan)

Total dissolved solids (TDS): 400 mL of esterification wastewater was filtered through a filtering system and the filtrate was dried in a constant temperature oven until the weight was constant.

Potential of hydrogen (pH): was measured by pH meter (PHS-3C, Shanghai REX Instrument Factory, China).

2.6.4. *Membrane performance in long term FO test*

The water flux (J_w) was calculated by the equation showed in section 2.4. The TOC rejection rate was used to show the pollutants rejection of membrane, which was calculated by the following equation [26,27]:

$$R = \left(1\text{-}\frac{C_p}{C_f}\right) \times 100\%$$

Where C_f (mg L^{-1}) is the TOC concentration before FO test in the feed solution, and the C_p (mg L^{-1}) is the TOC concentration of FO permeate, which can be estimated from the following:

$$C_\mathrm{p} = \frac{C_{d,e}\left(V_e + \Delta V\right) - C_{d,i} V_e}{\Delta V}$$

Where $C_{d,e}$ (mg L^{-1}) is the TOC concentration at the end of the test, $C_{d,i}$ is the initial TOC concentration in the draw solution with a volume of V_e (1 L), and (V (L) is the permeate water over 24 h. The water recovery R_e was calculated as following:

$$R_\mathrm{e} = \frac{\Delta V}{V_f} \times 100\%$$

where V_f (L) is the initial volume of feed solution.

Otherwise, the SEM images of membrane before and after the FO test were used to analysis the membrane fouling.

3. Results and discussion

3.1. *Effects of different solvents on membrane performance*

1,4-dixane, DMF, NMP were used as solvent respectively to prepare FO membranes (Table 1). As shown in Fig. 2, CTA membranes prepared from mixtures of CTA/DMF/lactic acid/PVP-K30 were found having the highest water flux and reverse salt flux (RSF), were 11.87 L m^{-2} h^{-1}, 88.48 g m^{-2} h^{-1} respectively. CTA membranes prepared by 1,4-dixane instead of DMF had lower water flux (9.52 L m^{-2} h^{-1}) and RSF (50.76 g m^{-2} h^{-1}). And the performance of membranes fabricated by NMP based dope solution fell somewhere in between.

Volatility and solubility of solvents was taken as reasons accounting for this phenomenon [16]. In generally, materials with lower boiling point were more volatile, compared with DMF and NMP, 1,4-dixane was more likely to volatilize from solution system owing to its lower boiling point. More solvent evaporation resulted in higher polymer content on the neonatal membrane surface. As the polymer content advanced, the macromolecule chains density went up [28], the collision and entanglement between polymer mol-

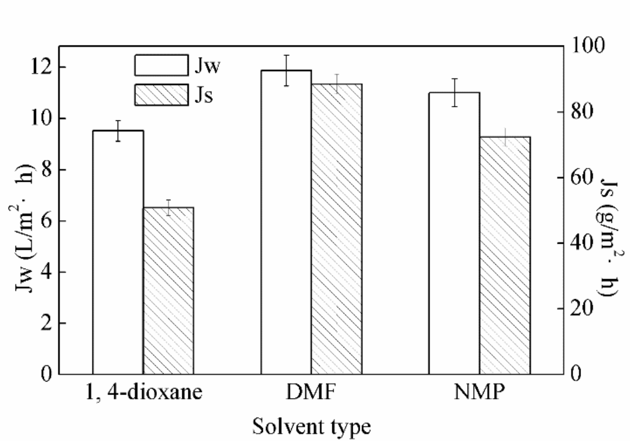

Fig. 2. Performance of FO membranes prepared with different types of solvent.

ecules reinforced, which lead to the dope solution viscosity increased [29]. Given this, it need take more time for water to diffuse into polymer matrix. Therefore, the gelation rate reduced and instantaneous demixing was translated into delayed demixing, which was in favor of developing denser membrane with higher selectivity [28].

Since the solubility parameter of CTA is closer to 1,4-dixane, there are higher affinities between CTA and 1,4-dixane than that between CTA and DMF (or NMP), resulting in that CTA tends to be more miscible in 1,4-dixane. For one thing, good miscibility of polymer in solvent may generate stronger bond energy, which hinders the exchange of solvent and nonsolvent in coagulation bath during phase separation. As a result, lower gelation velocity was achieved and membranes prepared under the circumstances were compact. For another, as 1,4-dixane was the good solvent of CTA, the strong solvation of CTA in 1,4-dixane made the macromolecular chain unfold freely [28], the gelation velocity declined consequently, so as to form the network pores having little aperture. As a result, the selectivity went up along with the permeability decreased.

Based on above analysis, 1,4-dixane was selected as the optimal solvent compared with the other solvent in term of water flux and salt rejection, and was used in the following studies.

3.2. Effects of CTA concentrations on membrane performance

Fig. 3 shows the performance of FO membranes prepared with CTA, 1,4-dioxane and lactic acid as membrane material, solvent and additive respectively. As the CTA concentration increased from 12.0 to 18.0 wt.%, the water flux decreased rapidly from 9.83 L m^{-2} h^{-1} to 5.44 L m^{-2} h^{-1}, the reverse salt flux was reduced to 17.33 g m^{-2} h^{-1} from 47.23 g m^{-2} h^{-1}. Membrane performance depends on the membrane structure on the premise of determining membrane material [29]. Cross-section and top surface SEM images of the FO membranes were shown in Fig. 4. Compared with membranes prepared from 14.0 wt.% CTA, the FO membranes cast from 16.0 wt.% CTA have smaller open-cell in macroporous support layer. And higher content of CTA produces smoother surface layer, which could more prone to resistant membrane fouling.

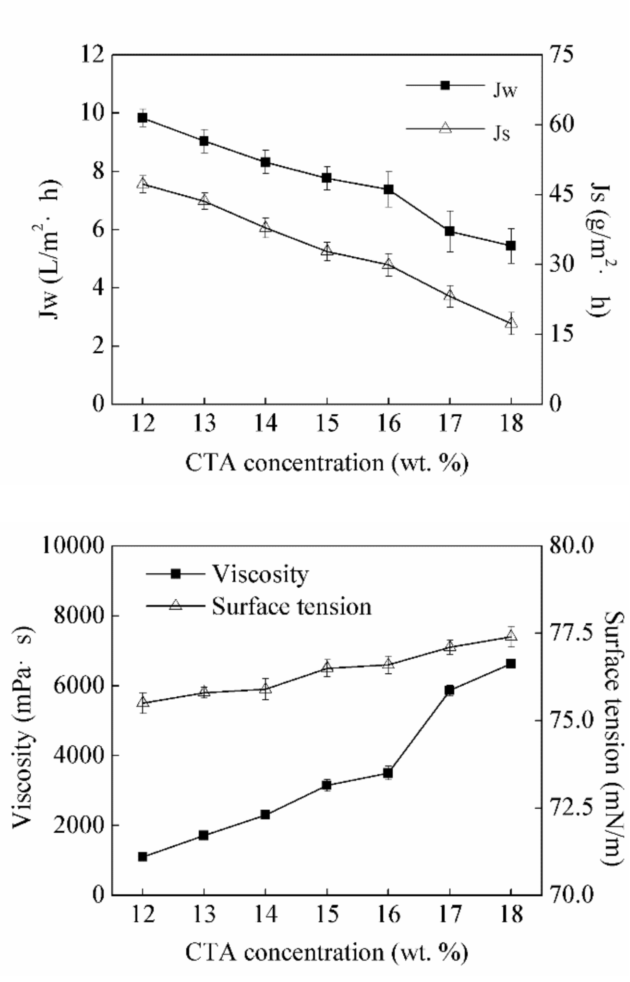

Fig. 3. Effects of CTA concentrations on membrane performance and dope solution performance.

Possible mechanisms related to thermodynamic and kinetic factors likely account for this the membrane structure. First, as the CTA concentration increased, the collision and entanglement between CTA molecules intensified, the macromolecule chains density in casting solution system increased [28], which generated denser skin layer accordingly, so that membrane selectivity was improved. Moreover, increasing polymer concentration improved viscosity of dope solution, which enhanced the flow resistance of dope solution. The casting solution surface tension also increased with the increase of the probability of collision and entanglement between polymer molecular (Fig. 3). Increased viscosity and surface tension severely hinder the exchange velocity between solvent and nonsolvent. The solvent has great difficulty evaporating into gelation bath, and the nonsolvent is hard to diffuse into casting solution. Delayed demixing resulted in the formation of dense membrane. To get the suitable permeability, selectivity and better performance stability, 15 wt.% CTA was used to prepare FO membranes.

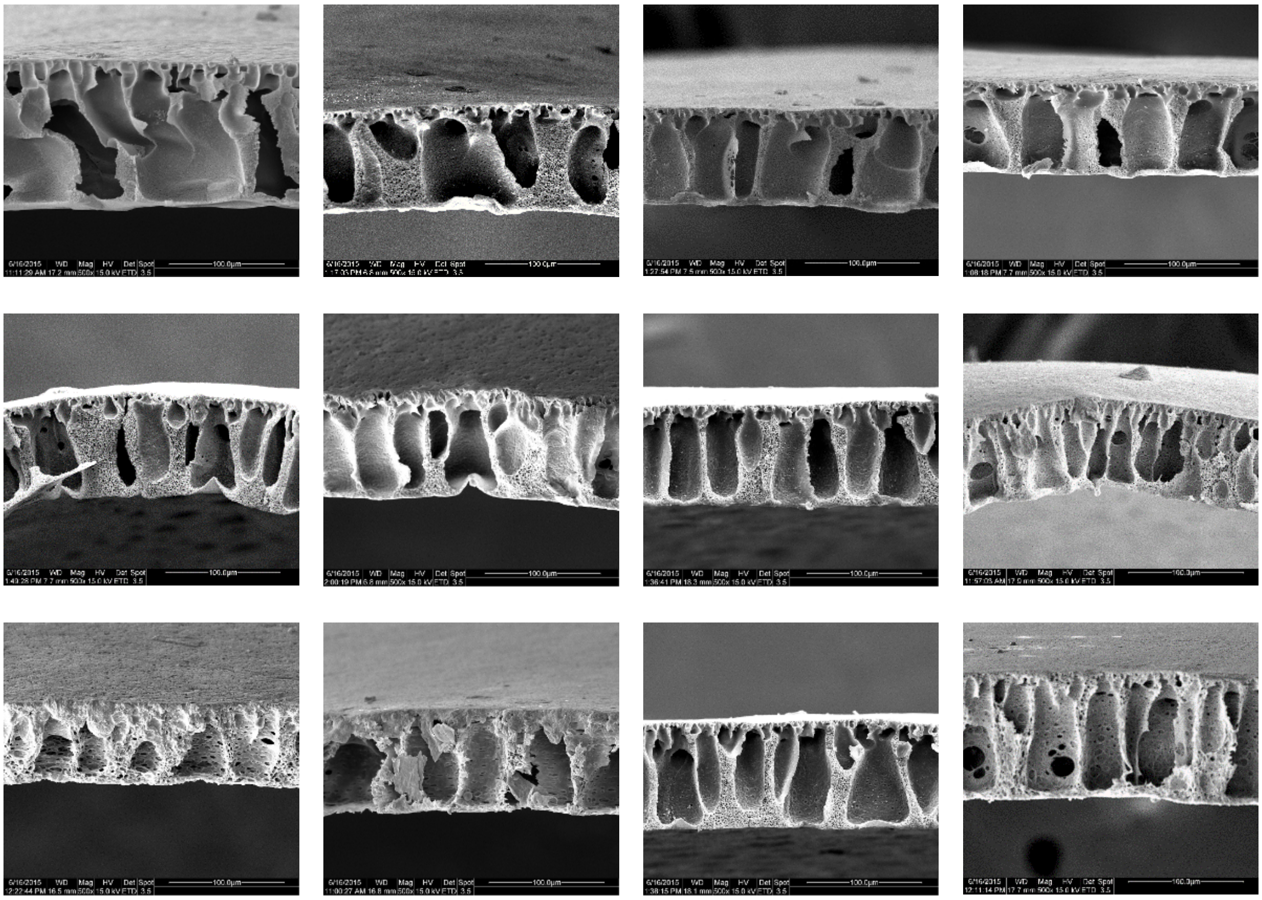

Fig. 4. Cross-section SEM images of different CTA concentrations and PVP-K30 concentrations. (a) 12 wt.% of CTA, (b) 13 wt.% of CTA, (c) 14 wt.% of CTA, (d) 15 wt.% of CTA, (e) 16 wt.% of CTA, (f) 17 wt.% of CTA, (g) 18 wt.% of CTA; (h) 1.0 wt.% of PVP-K30, (i) 1.5 wt.% of PVP-K30, (j) 2.0 wt.% of PVP-K30, (k) 2.5 wt.% of PVP-K30, (l) 3.0 wt.% of PVP-K30.

3.3 Effects of different additives on membrane performance

In order to improve the water flux of FO membranes, lactic acid and PVP-K30 are used as additives to prepare membranes in this study. As shown in Fig. 5, with the lactic acid content increased from 0 to 6.0 wt.%, the water flux and RSF went up significantly, the water flux of membranes increased more rapidly especially when the concentration of lactic acid increase to 1.0 wt.% from 0. Therefore, lactic acid used alone as additives played a great role in improving membrane performance. When lactic acid concentration was 4.0 wt.%, the membrane with better performance was obtained based on the balance between water flux and RSF.

Lactic acid acted as a low-molecular-weight organic acid has hydrophilic groups (–OH and –COOH), which induces the hydrogen bond formation of hydrogen atom of lactic acid and the oxygen atom in the 1,4-dioxane, a high hydrophilic groups is formed. Besides, there are oxygen atoms in CTA molecules, which can combine hydrogen atoms of the hydroxyl groups and carboxyl groups, and form hydrogen bonds. Since the instability of hydrogen bonds, the thermodynamics stability of casting solution reduces. So, increasing amount of lactic acid lead to more hydrogen bonds formed and accelerated the exchange rate between coagulation bath and casting solution [30]. Furthermore, the casting solution viscosity and surface tension dropped off with the increasing of lactic acid concentration, which reduces the mass transfer resistance between molecules, raised the rate of solvent removing out from dope solution. These two effects both speeded up the gelation velocity, porous and loose membrane with higher water flux was obtained eventually.

In the premise of determining the lactic acid concentration, PVP-K30 acted as pore-forming agent was used for membrane preparation. It indicated in Fig. 5 that the water flux and RSF increased 55.05 and 220.7% respectively with the increasing of PVP-K30 content from 1.0 to 3.0 wt.%.

As a swelling agent, PVP-K30 dissolved in solvent, which was equivalent to compete with polymer for solvent. Thus, with the increasing of PVP-K30, the salvation of CTA with solvent decreased, the crimp ratio of macromolecule chains increased, and the interactions between polymer chain segments diminished, and the aggregation pores and liquid-liquid interfacial phase micro-void with large aperture were obtained [28]. In addition, the hydrophilic characteristic of PVP-K30 could enhance the affinity between gelation bath and dope solution, so when more PVP-K30 was added to casting solution, the exchange rate between solvent and non-solvent would speed up, which lead to the advancing gelation rate. Therefore, these two effects were favor to form loose and porous membrane, and induced bigger

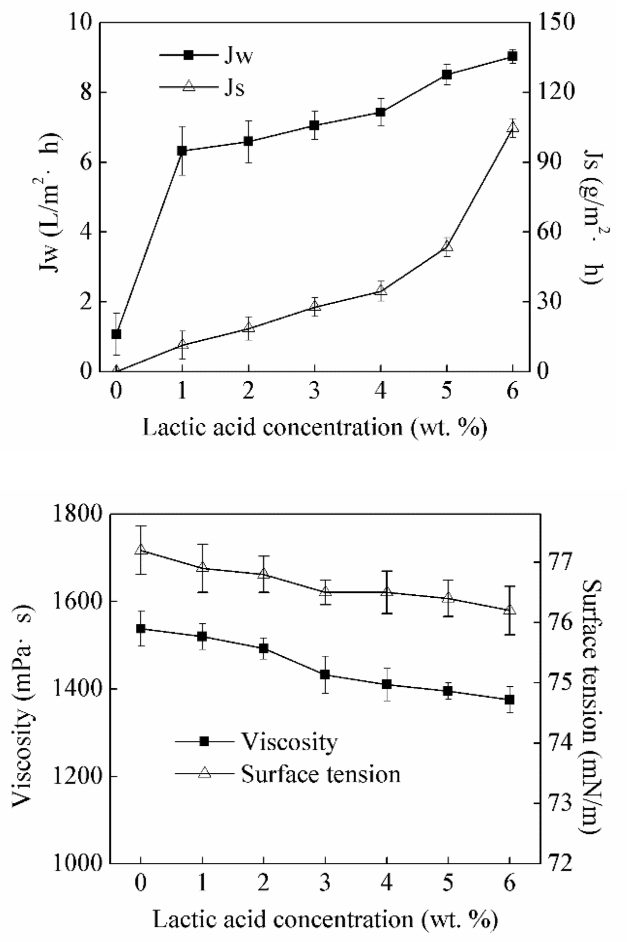

Fig. 5. Effects of lactic acid concentration on membrane performance and dope solution performance.

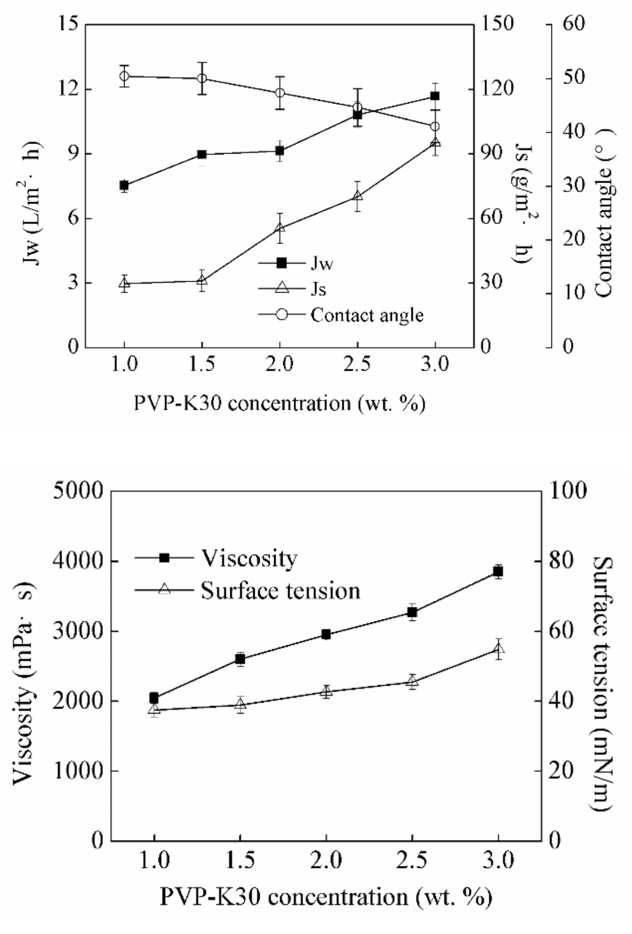

Fig. 6. Effects of PVP-K30 concentration on membrane performance and dope solution performance.

water flux and RSF. On the other hand, however, along with the increasing PVP-K30, the dope solution viscosity and surface tension increased, which consequently restrain the movement of macromolecule chains, the exchange rate between solvent and non-solvent decreased, as a result, it tends to form a compact structure.

Above two mechanisms suppressed each other and jointly affect the formation of membrane structure. Here, the factors that generated looser and more porous membranes played a dominant role. Besides, it also indicated (Fig. 6) that the addition of PVP-K30 improved the hydrophilicity of CTA membrane. This is one of the reasons which resulted in increased water flux. As shown in Fig. 4, as the PVP-K30 content went up, larger pores and more porous membrane were formed. Compared with the date in Fig. 5, the RSF was lower at same water flux, which revealed that the membranes prepared by PVP-K30 had better selectivity. When PVP-K30 concentration was 1.5 wt.%, the membrane was desirable based on the balance between water flux and RSF, and the optional membrane was applied for treating esterification wastewater.

Fig. 7 demonstrates the gelation distance of casting solution with different additives. It is observed that the gelation front advanced forward with time. Along with the time, gelation distance increased at different rates. Two additive combinations had roughly same trend. Before 1.0 s, the gelation velocity increased most rapidly, and gradually descended afterwards until reached phase equilibria. Within 1.0 s, the gelation velocities of both were almost equal. And whereafter, the gelation rate of 3.0 wt.% lactic acid and 1.5 wt.% PVP-K30 was larger than that of 3.0 wt.% lactic acid, which explained the membranes prepared from 3.0 wt.% lactic acid and 1.5 wt.% PVP-K30 were looser and more porous. It was consistent with the results of Figs. 5, 6 showed.

3.4. Application of CTA FO membrane to treat esterification water

Through the comparison for the solvent type, CTA concentration and additives concentrations, the optional composition of casting solution was determined as 15.0 wt.% CTA, 80.5 wt.% 1,4-dioxane, 3.0 wt.% lactic acid and 1.5 wt.% PVP-K30. The optional membrane was utilized to treat esterification wastewater [31].

The long-term running performance and fouling properties of developed CTA membranes under the FO mode

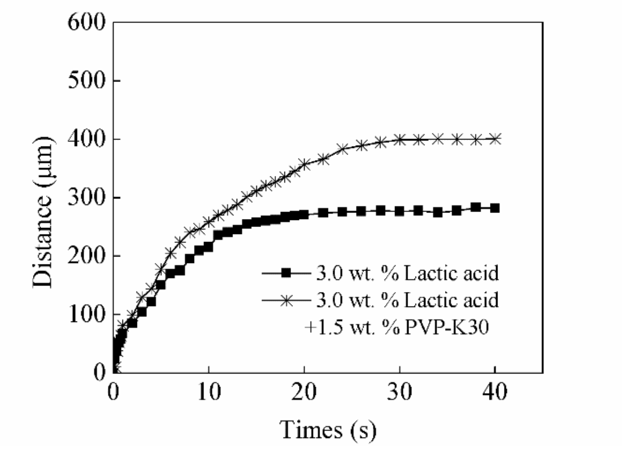

Fig. 7. Gelation kinetics curves using different additives.

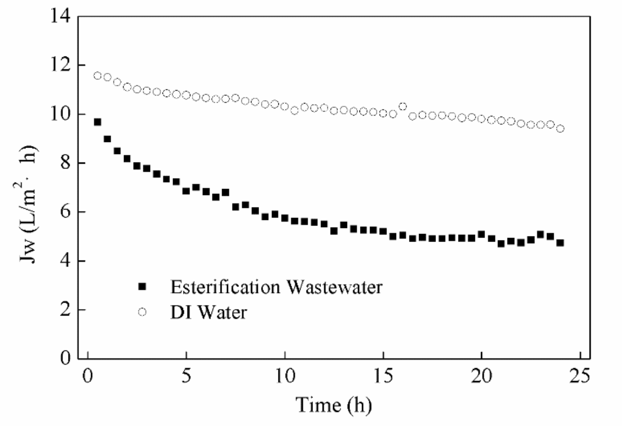

Fig. 8. Water flux of FO membrane measured in a 24-hour lasting test (DS: 2 M NaCl; flow velocity: 0.3 L min^{-1}; feed solution: DI water or 1 L of pre-treatment effluent).

were further studied. As shown in Fig. 8, the initial water flux were around 11.56 L m^{-1} h^{-1} and 9.40 L m^{-1} h^{-1} when the feed solution were DI water and esterification wastewater, respectively. Since the draw solution was maintained at 2 M NaCl throughout the both long-term test over 24 h containing baseline test and actual test, the baseline curves showed a slightly reduction of 18.7%. This little change was attributed to RSF and internal concentration polarization (ICP) effects [32]. Whereas, the water flux went down significantly by 55 % in the actual experiment. Compared to the baseline, except the RSF and ICP effects, membrane fouling was also regarded as one of the reasons for water flux declination. Especially in the early 5 h, the flux declined sharply from 9.56 L m^{-1} h^{-1} to about 6.0 L m^{-1} h^{-1}, which was probably because of the cake layer generated by contaminants on the membrane surface or the pore blocking due to the small pollutants particles (Fig. 8). And after 5 h, the water flux reduced slowly since the membrane fouling become to stability [33].

After 24-hour continuous treatment, the water recovery reached to 57.1%. The FO process brought a high pollutants rejection efficiency with TOC rejection up to 96.5% (Table 3). However, it was noticing that, there still existed a larger TOC concentration after the FO process (Table 2), the reasons for this phenomenon could be that the poor density of membrane skin layer gave small organic molecules a pass, and this kind of wastewater contained a lot of such small molecules, for example, 1,3-propanediol, glycerol, ethylene glycol etc. Even so, the molecular of 1,3-propanediol, glycerol and ethylene glycol was all larger than that of Na^+ and Cl^-, denser membranes would be more capable to achieve a quite high TOC rejection. Besides, the TDS in the FO concentrated solution should have been as 2.33 times as initial concentration, but the actual TDS concentration exceeded 2.33 times of initial concentration due to the reverse salt flux.

4. Conclusions

Compared with NMP and DMF, CTA FO membranes prepared from 1,4-dixane possessed more selectivity, leading to lower water flux. With the increasing polymer content, the water flux and RSF showed a gradual reduced

Table 2
Concentration of raw wastewater and properties of FO process streams (pre-treatment effluent, FO concentration, initial draw solution and draw solution at the end of test and FO permeate)

Properties	TOC (mg L^{-1})	TDS (mg L^{-1})	pH
Raw wastewater	49800	295	3.69
Pre-treatment effluent (C_f)	39420	284	7.30
FO concentration	91000	2380	7.48
Initial draw solution ($C_{d,i}$)	2.76	–	7.67
Draw solution at the end of the test ($C_{d,e}$)	509.00	–	7.35
FO permeate (C_p)	1395.58	–	7.35

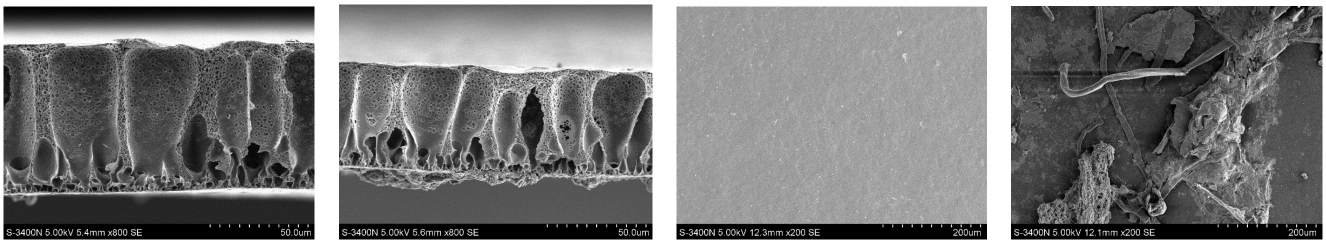

Fig. 9. Surface and cross-section SEM images of virgin membrane (a, c) and fouled membrane (b, d).

Table 3
Performance of FO membranes for esterification wastewater (DS: 2 M NaCl; flow rate: 0.3 L min^{-1})

Feed solution	Initial flux (L m^{-2}·h^{-1})	Final flux (L m^{-2}·h^{-1})	Reduction rate of flux (%)	Pollutants rejection R (%)	Water recovery R_e (%)
Esterification wastewater	9.67	4.73	51.1	96.5	57.1

tendency. More lactic acid as additives added into dope solution produced looser and more porous membranes. Addition of PVP-K30 also improved membrane permeability, instead, the selectivity dropped off with it. In order to achieve better permeability and selectivity, 15.0 wt.% CTA, 80.5 wt.% 1,4-dixane, 3.0 wt.% lactic acid, 1.5 wt.% PVP-K30 were used for making up the optional dope solution. For the long-term test, the water flux went down significantly by 51.1%, especially in the early 5 h, the flux declined sharply from 9.56 L m^{-1} h^{-1} to about 6.0 L m^{-1} h^{-1}, and then the water flux reduced slowly since the membrane fouling become to stability. FO treatment brought about 57.1% of water recovery and favorable pollutants rejection with TOC rejection exceeding 96%. The application of CTA FO membranes to treat esterification wastewater was feasible.

Acknowledgments

This work was financially supported by “the National Science Foundation of China (Grant No. 21376030)”.

References

[1] P. Roslev, K. Vorkamp, J. Aarup, K. Frederiksen, N. Ph. Degradation of phthalate esters in an activated sludge wastewater treatment plant. Water Res., 41 (2007) 969–976.

[2] K. Wu, X.H. Zhou, Y.B. Wang, W.C. Zhou. Research progress of treatment method for polyester production wastewater. Chem. Propell. Polym. Mater., 7 (2009) 26–30.

[3] X.Z. Feng. Method analysis for treating esterification wastewater. Sci. Tech. Inform., (2012) 139–139.

[4] S.F. Wu. Influential factors on COD of esterification waste water from polyester plant. China Syn. Fiber Ind., 36 (2013) 61–63.

[5] S. Zhao, L. Zou, C.Y. Tang, D. Mulcahy. Recent developments in forward osmosis: Opportunities and challenges. J. Membrane Sci., 396 (2012) 1–21.

[6] T.S. Chung, S. Zhang, K.Y. Wang, J. Su, M.M. Ling. Forward osmosis processes: Yesterday, today and tomorrow. Desalination, 287 (2012) 78–81.

[7] D.L. Shaffer, J.R. Werber, H. Jaramillo, S. Lin, M. Elimelech. Forward osmosis: Where are we now? Desalination, 356 (2015) 271–284.

[8] Y. Cui, X.Y. Liu, T.S. Chung, Enhanced osmotic energy generation from salinity gradients by modifying thin film composite membranes, Chem. Eng. J., 242 (2014) 195–203.

[9] B.D. Coday, P. Xu, E.G. Beaudry, J. Herron, K. Lampi, N.T. Hancock, T.Y. Cath. The sweet spot of forward osmosis: treatment of produced water, drilling wastewater, and other complex and difficult liquid streams. Desalination, 333 (2014) 23–35.

[10] A.Y. Gebreyohannes, E. Curcio, T. Poerio, R. Mazzei, G.D. Profio, E. Drioli, L. Giorno. Treatment of olive mill wastewater by forward osmosis. Sep. Purif. Technol, 147 (2015) 292–302.

[11] P. Zhao, B. Gao, Q. Yue, H.K. Shon. The performance of forward osmosis process in treating the surfactant wastewater: the rejection of surfactant, water flux and physical cleaning effectiveness. Chem. Eng. J., 281 (2015) 688–695.

[12] P. Zhao, B. Gao, Q. Yue, H.K. Shon, P. Liu, Q. Yue. Explore the forward osmosis performance using hydrolyzed polyacrylamide as draw solute for dye wastewater reclamation in the long-term process. Chem. Eng. J., 273 (2015) 316–324.

[13] R. Kumar, P. Pal. A novel forward osmosis-nano filtration integrated system for coke-oven wastewater reclamation. Chem. Eng. Res. Des., 100 (2015) 542–553.

[14] Y. Dong, Z. Wang, C. Zhu, Q. Wang, J. Tang, Z. Wu. A forward osmosis membrane system for the post-treatment of MBR-treated landfill leachate. J. Membrane Sci., 471 (2014) 192–200.

[15] X. Zhang, Z. Ning, D.K. Wang, J.C.D.D. Costa. Processing municipal wastewaters by forward osmosis using CTA membrane. J. Membrane Sci., 468 (2014) 269–275.

[16] T.P.N. Nguyen, E.T. Yun, I.C. Kim, Y.N. Kwon. Preparation of cellulose triacetate/cellulose acetate (CTA/CA)-based membranes for forward osmosis. J. Membrane Sci., 433 (2013) 49–59.

[17] M. Sairam, E. Sereewatthanawut, K. Li, A. Bismarck, A.G. Livingston. Method for the preparation of cellulose acetate flat sheet composite membranes for forward osmosis-Desalination using $MgSO_4$ draw solution. Desalination, 273 (2011) 299–307.

[18] N.Y. Yip, A. Tiraferri, W.A. Phillip, J.D. Schiffman, M. Elimelech. High performance thin-film composite forward osmosis membrane. Env. Sci. Tec. 44 (2010) 3812–3818.

[19] L. Setiawan, R. Wang, K. Li, A.G. Fane. Fabrication of novel poly (amide-imide) forward osmosis hollow fiber membranes with a positively charged nanofiltration-like selective layer. J. Membrane Sci., 369 (2011) 196–205.

[20] D. Emadzadeh, W.J. Lau, T. Matsuura, M. Rahbari-Sisakht, A. F. Ismail. A novel thin film composite forward osmosis membrane prepared from PSf-TiO_2 nanocomposite substrate for water desalination. Chem. Eng. J., 237 (2014) 70–80.

[21] J. Su, Q. Yang, J.F. Teo, T.S. Chung, Cellulose acetate nanofiltration hollow fiber membranes for forward osmosis processes, J. Membr. Sci. 355 (2010) 36–44.

[22] C.O. Rui, T.S. Chung. Fabrication and positron annihilation spectroscopy (PAS) characterization of cellulose triacetate membranes for forward osmosis. J. Membrane Sci., 394–395 (2012) 230–240.

[23] Y. Cui, Q. Ge, X.Y. Liu, T.S. Chung*, Novel forward osmosis process to effectively remove heavy metal ions, J. Membr. Sci. 467 (2014) 188–194.

[24] Y. Cui, X.Y. Liu, T.S. Chung, M. Weber, C. Staudt, C. Maletzko, Removal of organic micro-pollutants (phenol, aniline and nitrobenzene) via forward osmosis (FO) process: Evaluation of FO as an alternative method to reverse osmosis (RO), Water Res., 91 (2016) 104–114.

[25] J. Ji, Y. Yun, Z. Zeng, R. Wang, X. Zheng, L. Deng, C. Li. Preparation and arsenic adsorption assessment of PPESK ultrafiltration membranes with organic/inorganic additives. Appl. Surf. Sci., 351 (2015) 715–724.

[26] Y. Yu, S. Seo, I.C. Kim, S. Lee. Nanoporous polyethersulfone (PES) membrane with enhanced flux applied in forward osmosis process. J. Membrane Sci., 375 (2011) 63–68.

[27] J. Su, R.C. Ong, P. Wang, T.S. Chung, B.J. Helmer, J.S. de Wit, Advanced FO membranes from newly synthesized CAP polymer for wastewater reclamation through an integrated FO-MD hybrid system. AIChE J. 59 (2012) 1245–1254.

[28] P. Qin, X. Hong, M.N. Karim, T. Shintani, J. Li, C. Chen. Preparation of poly (phthalazinone-ether-sulfone) sponge-Like ultrafiltration membrane. Langmuir, 29 (2013) 4167–4175.

[29] B. Sui. Effect of thermodynamic and kinetic factors on structure and performance of asymmetric membrane formed via L-S phase inversion. Membrane Sci. Tech., 31 (2011) 1–11.
[30] L.L. Li, D. Wang. Preparation and performance of cellulose acetate forward osmosis membrane. J. Funct. Mater., 43 (2012) 595–598.
[31] S. Pandian, A.R. Katha, J.H. Moon, S.M. Kolake, S. Han. Exploring the effect of additives on polyamide membrane surface for seawater desalination using density functional tools. Desalination, 367 (2015) 28–36.
[32] W.C.L. Lay, J. Zhang, C. Tang, R. Wang, Y. Liu, A.G. Fane. Factors affecting flux performance of forward osmosis systems. J. Membrane Sci., 394–395 (2012) 151–168.
[33] Z. Wang, J. Tang, C. Zhu, Y. Dong, Q. Wang, Z. Wu. Chemical cleaning protocols for thin film composite (TFC) polyamide forward osmosis membranes used for municipal wastewater treatment. J. Membrane Sci., 475 (2015) 184–192.